V13D 2892

Duration of convergence at the Pacific-Gondwana plate margin: Insights from accessory phase petrochronology of the Alpine Schist, New Zealand

Sophie Briggs , John Cottle , Matthijs Smit , Nicole Arnush[1]

[1]Department of Earth Science, University of California Santa Barbara
sbriggs@umail.ucsb.edu

[2]Pacific Center for Isotope and Geochemical Research, Department of Earth, Ocean and Atmospheric Sciences, University of British Columbia, Vancouver, Canada. msmit@eos.ubc.ca

Background

- The Alpine Schist provides a unique opportunity to investigate the geodynamic processes involved in the genesis of microcontinents such as Zealandia.
- Although the metamorphosed accretionary complex was long thought to record Jurassic – Cretaceous subduction at the eastern Gondwana margin, recent Lu-Hf garnet geochronology has resolved prograde ages as young as 75 Ma.
- Young prograde ages post-date the cessation of Pacific-Gondwana subduction (~105 Ma) and record prolonged convergence at the margin, while adjacent areas record extension and detachment of the Zealandia microcontinent.
- This study uses LASS-ICP-MS depth-profiling of metamorphic zircon overgrowths to constrain the duration of this late-stage convergence at the Gondwana margin.

Fig. 1: Zealandia bathymetry shows 90% of the microcontinent is submerged. Continental arc and accretionary complex assemblages are highlighted in purple and pink. The Alpine Schist accretionary complex is well exposed in the Southern Alps due to uplift and exhumation along the active plate boundary that traverses the South Island [9].

Fig. 2: Reconstruction of the Pacific - eastern Gondwana continental margin showing along-strike continuation of continental arc assemblages. Hikurangi Plaetau (green) arrived at the margin at ~108 - 105 Ma [10].

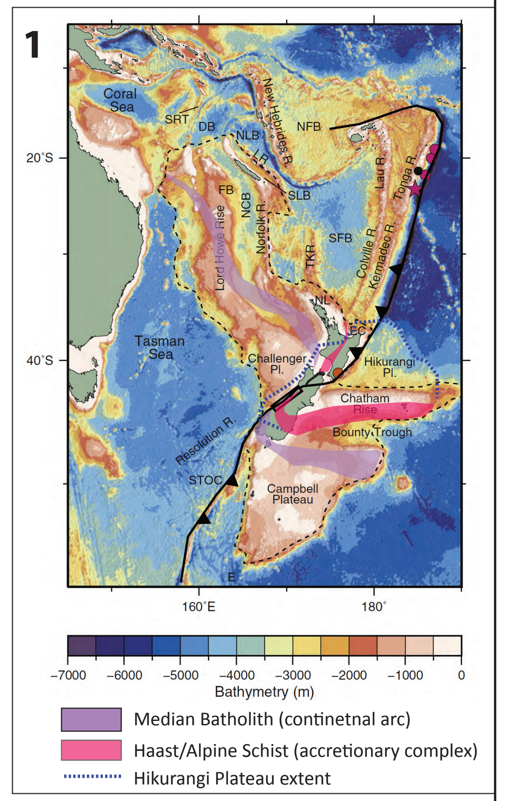

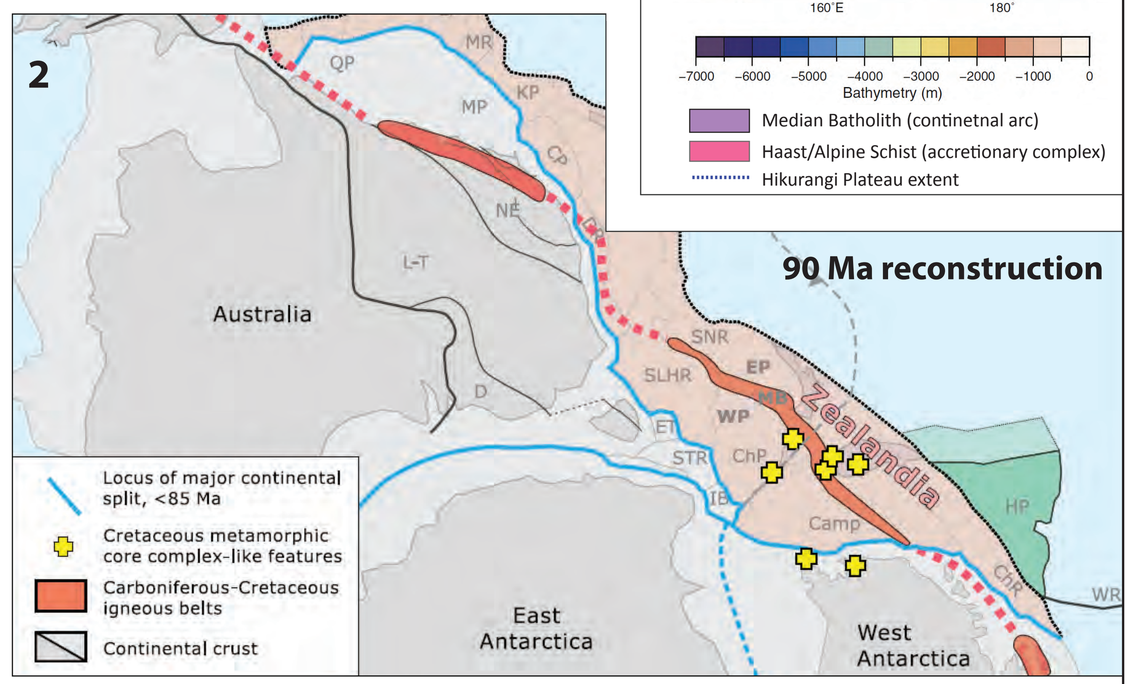

Lu-Hf garnet geochronology

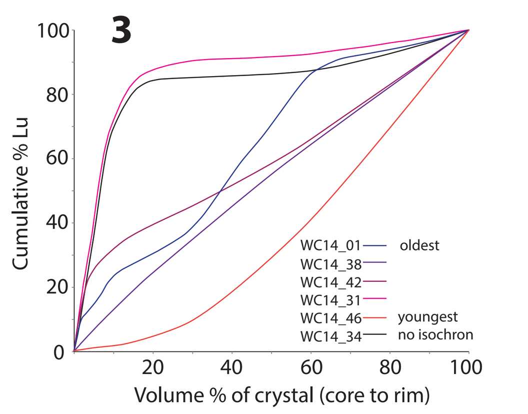

Fig. 3: The multi-grain bulk dissolution Lu-Hf garnet geochronology technique produces a 'mean' age for protracted garnet growth. The distribution of parent isotope [176]Lu through the garnet grain volume determines the age bias toward core or rim.

Fig. 4: Variation in garnet ages reflects progressive fold-thrust deformation in the accretionary complex.

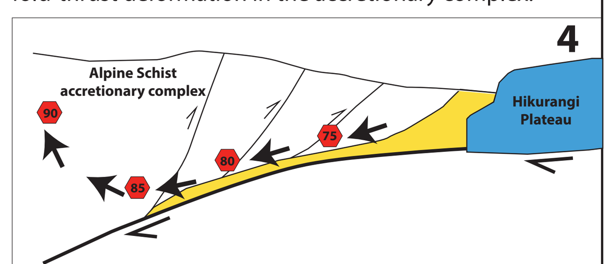

Acknowledgements

Thanks to Andrew Kylander-Clark, Gareth Seward, and Joshua Garber for input and assistance in the lab.

References

[1,3] Mortimer, N., & Cooper, A. F. (2004). U-Pb and Sm-Nd ages from the Alpine Schist, New Zealand. New Zealand Journal of Geology and Geophysics, 47(1), 21-28.
[2] Cooper, A. F., & Ireland, T. R. (2015). The Pounamu terrane, a new Cretaceous exotic terrane within the Alpine Schist, New Zealand; tectonically emplaced, deformed and metamorphosed during collision of the LIP Hikurangi Plateau with Zealandia. Gondwana Research, 27(3), 1255-1269.
[4] Briggs, S. I., Cottle, J. M., Hagen-Peter, G. A. (2014). Combined U-Th-Pb monazite and Lu-Hf garnet ages from the Alpine Schist: Implications for the timing and duration of Barrovian metamorphism in the Southern Alps, New Zealand. GSA Abstracts with Programs, 46 (6): 140
[5] Scott, J. M., Auer, A., Muhling, J. R., Czertowicz, T. A., Cooper, A. F., Billia, M. A., & Kennedy, A. K. (2015). New P–T and U–Pb constraints on Alpine Schist metamorphism in south Westland, New Zealand. New Zealand Journal of Geology and Geophysics, 58(4), 385-397.
[6] Cooper, A. F., & Ireland, T. R. (2013). Cretaceous sedimentation and metamorphism of the western Alpine Schist protoliths associated with the Pounamu Ultramafic Belt, Westland, New Zealand. New Zealand Journal of Geology and Geophysics, 56(4), 188-199.
[7, 8] Vry, J. K., Baker, J., Maas, R., Little, T. A., Grapes, R., & Dixon, M. (2004). Zoned (Cretaceous and Cenozoic) garnet and the timing of high grade metamorphism, Southern Alps, New Zealand. Journal of Metamorphic Geology, 22(3), 137-157.
[9] Matthews, K. J., Williams, S. E., Whittaker, J. M., Müller, R. D., Seton, M., & Clarke, G. L. (2015). Geologic and kinematic constraints on Late Cretaceous to mid Eocene plate boundaries in the southwest Pacific. Earth-Science Reviews, 140, 72-107.
[10] Mortimer, N. (2008). Zealandia. ASEG Extended Abstracts, 2006(1), 1-4.
[11] Cottle, J. M., Horstwood, M. S. A., & Parrish, R. R. (2009). A new approach to single shot laser ablation analysis and its application to in situ Pb/U geochronology. Journal of Analytical Atomic Spectrometry, 24(10), 1355-1363.
[12] Rubatto, D., & Hermann, J. (2007). Experimental zircon/melt and zircon/garnet trace element partitioning and implications for the geochronology of crustal rocks. Chemical Geology, 241(1), 38-61.
[13] Hermann, J., & Rubatto, D. (2003). Relating zircon and monazite domains to garnet growth zones: age and duration of granulite facies metamorphism in the Val Malenco lower crust. Journal of Metamorphic Geology, 21(9), 833-852.
[14] Rubatto, D., Hermann, J., & Buick, I. S. (2006). Temperature and bulk composition control on the growth of monazite and zircon during low-pressure anatexis (Mount Stafford, central Australia). Journal of Petrology, 47(10), 1973-1996.
[15] Rubatto, D. (2002). Zircon trace element geochemistry: partitioning with garnet and the link between U–Pb ages and metamorphism. Chemical Geology, 184(1), 123-138.
[16] Rey, P. F., & Müller, R. D. (2010). Fragmentation of active continental plate margins owing to the buoyancy of the mantle wedge. Nature Geoscience, 3(4), 257-261.

Geochronology synthesis

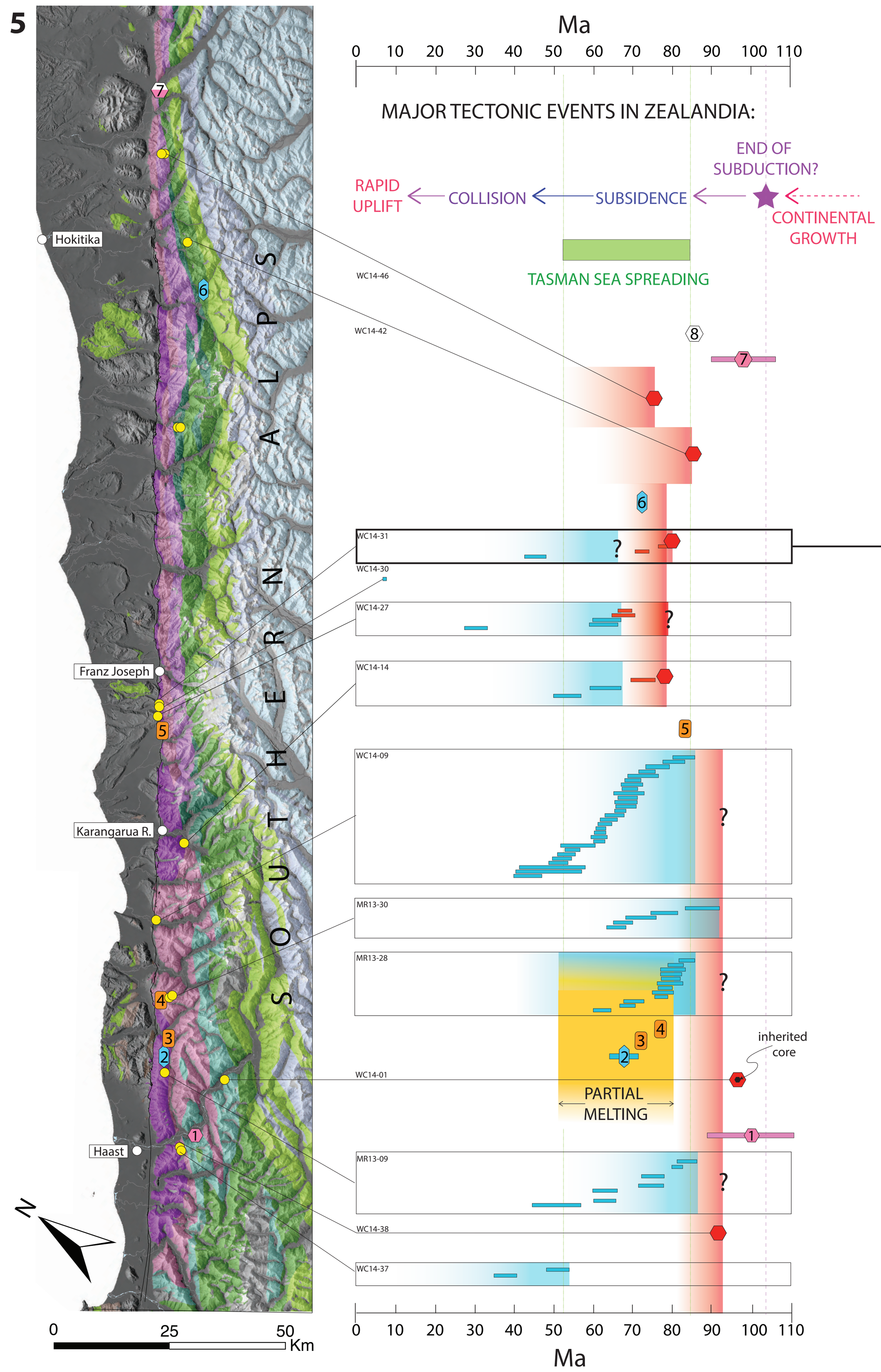

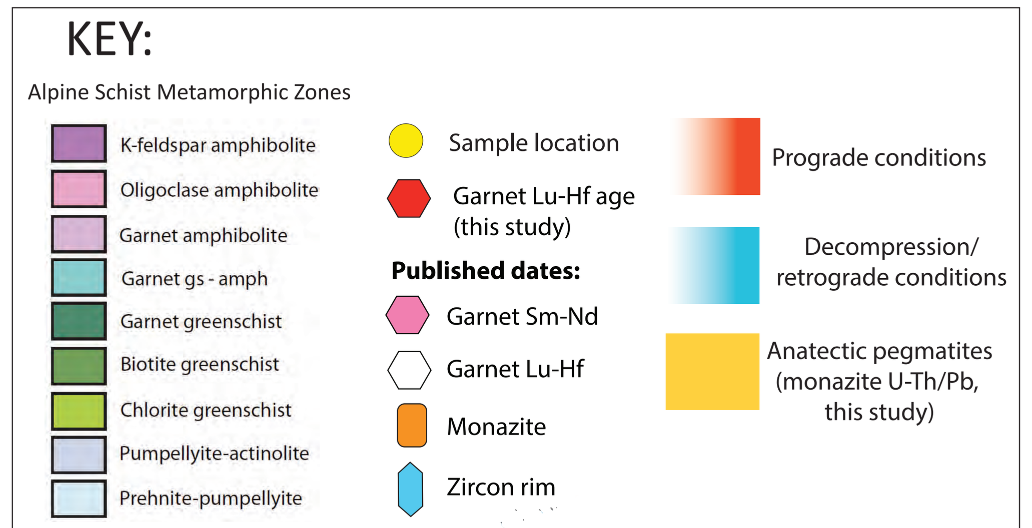

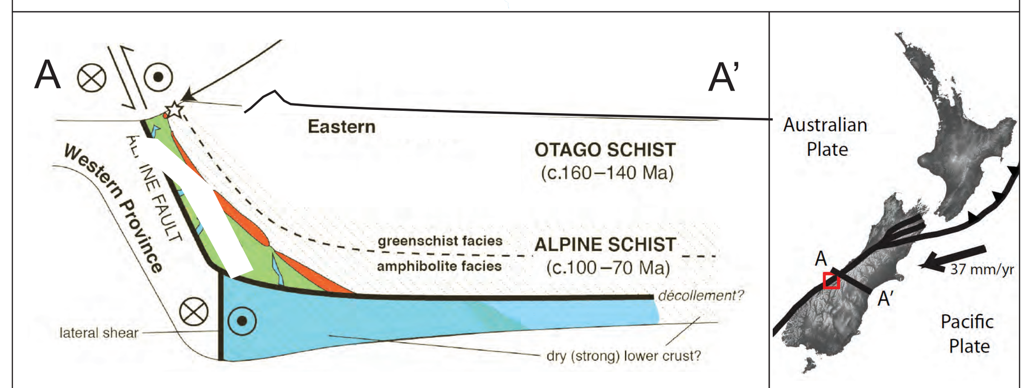

Dating prograde conditions: garnet-stable zircon rims

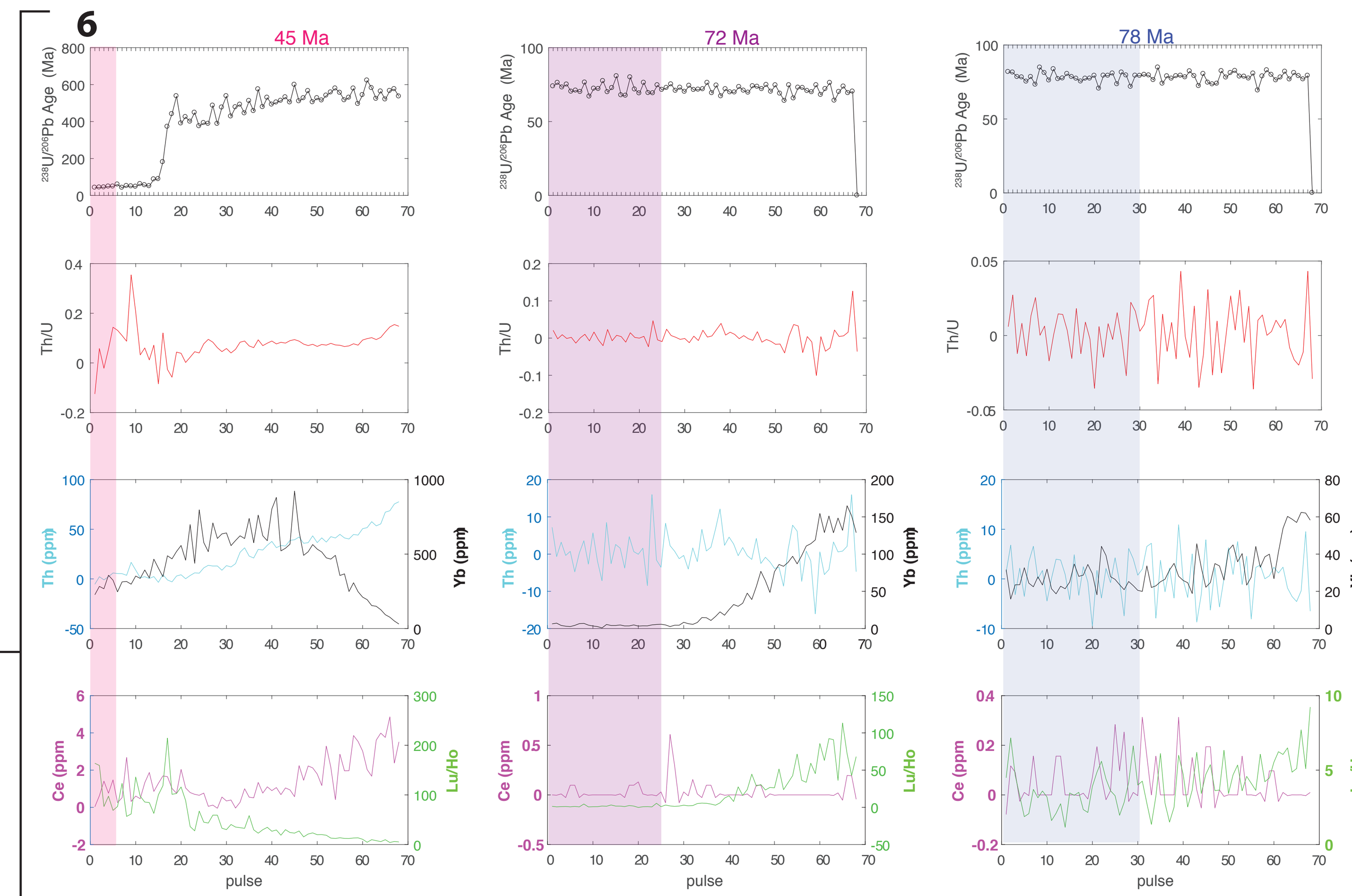

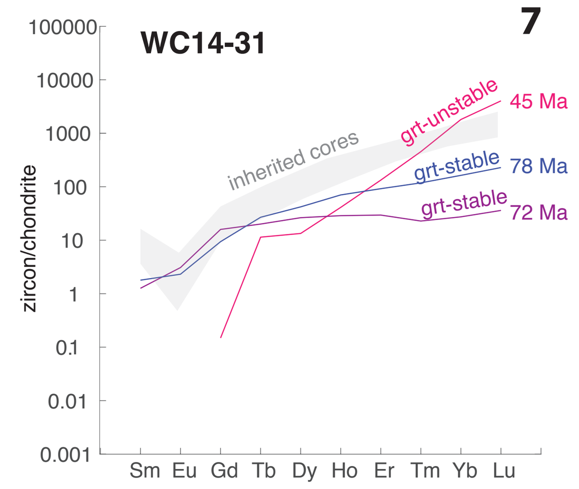

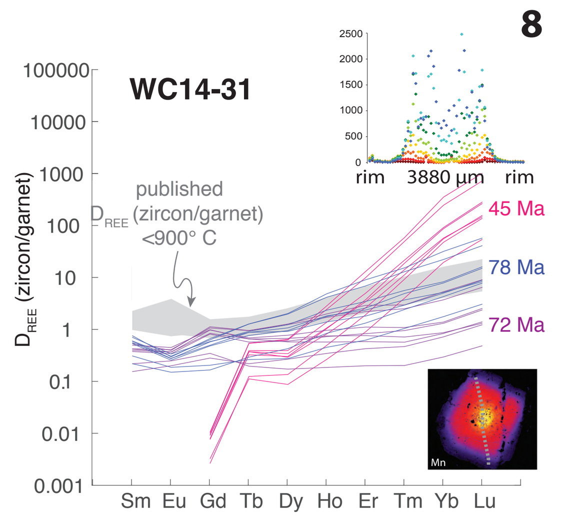

- HREE profiles used to differentiate between zircon formed during garnet-stable conditions, and zircon formed in the presence of melt/fluid or during garnet breakdown (Fig. 7).
- The corresponding U-Pb zircon ages are consistent with the timing of garnet growth and partial melting determined independently by Lu-Hf garnet geochronology and U-Th/Pb monazite from anatectic pegmatites (Fig. 5).
- U-Pb zircon data span the transition from garnet growth to garnet resorption and can be used to corroborate bulk or 'mean' Lu-Hf garnet ages where garnet grew over protracted timescales.
- Comparison of zircon and garnet REE compositions provides estimates of DREE (zircon/garnet) for quartzofeldspathic compositions at greenschist – amphibolite conditions. (Fig. 8).

Fig. 8: D_{REE} (zircon/garnet) calculated using average zircon rim REE concentrations for each age population and the first 8 rim analyses from garnet REE transect in top right. Published D's shown in gray are from [12], [13], [14], [15].

Dating decompression/melting/retrograde conditions

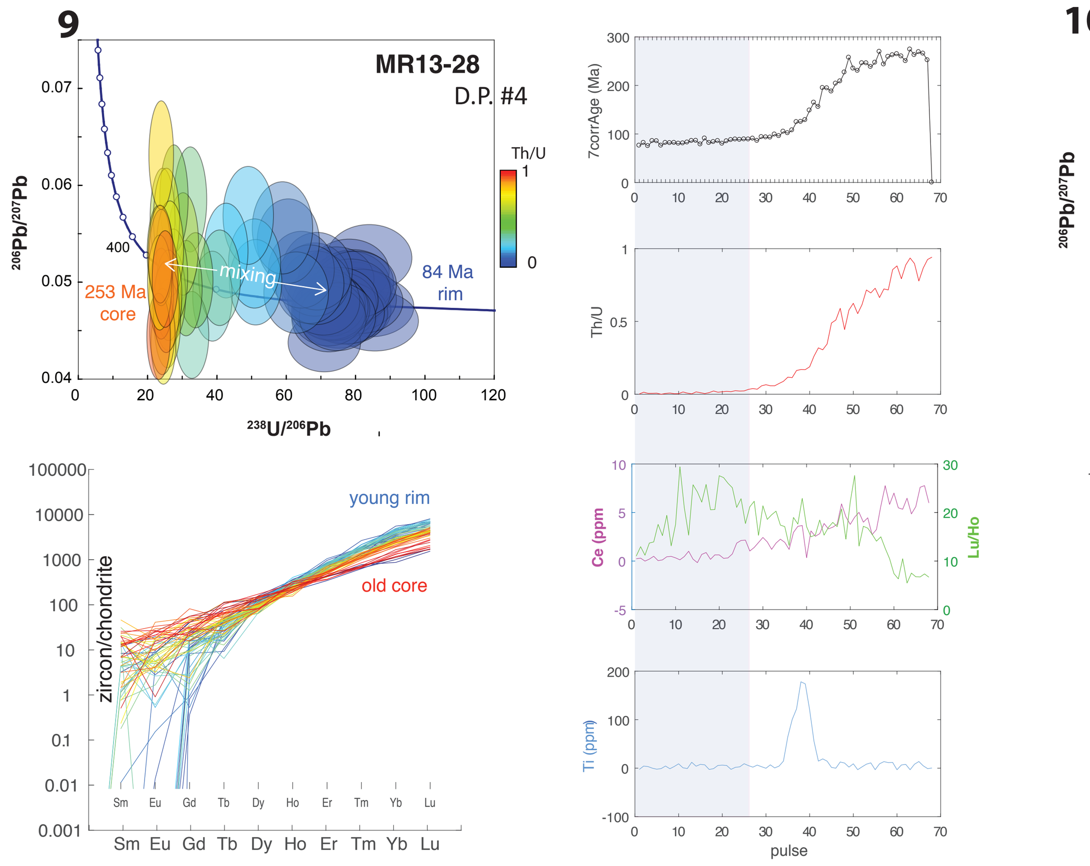

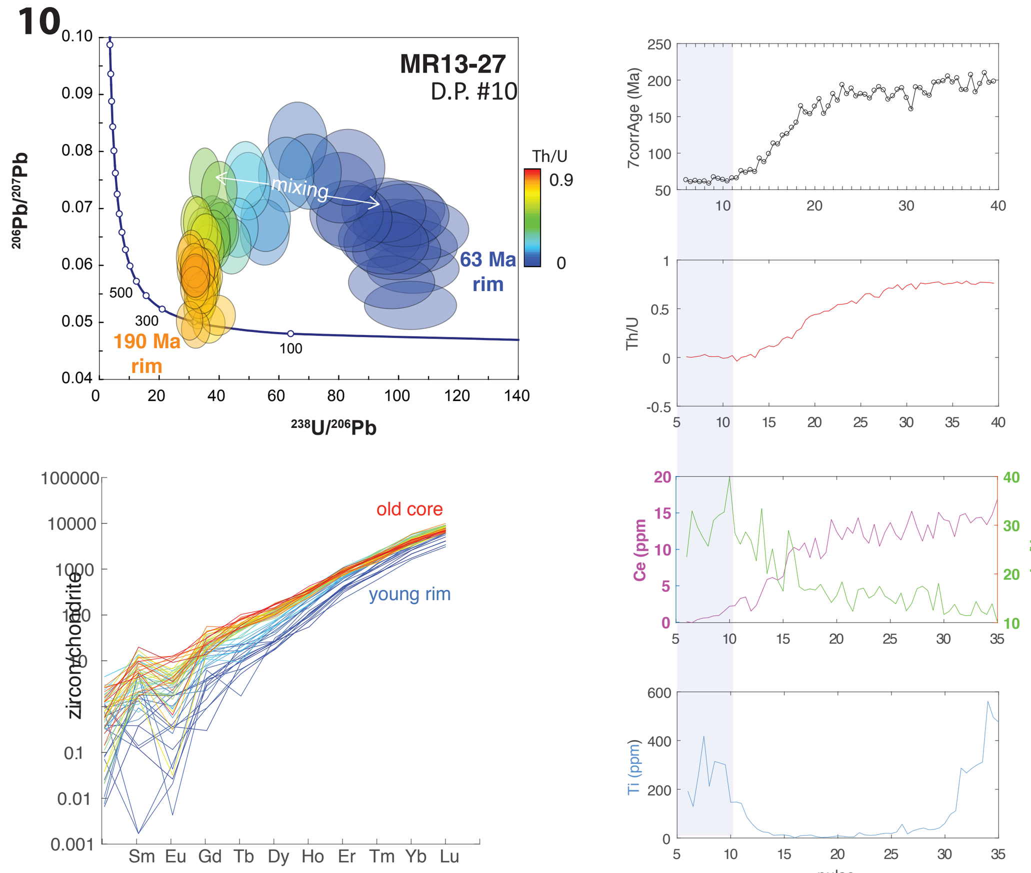

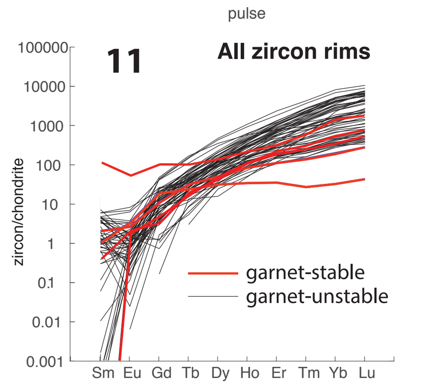

- Thin (<8 μm) metamorphic zircon overgrowths are easily distinguished from igneous cores based on Th/U (<<1) and distinct enrichment/depletion in HREE (Fig. 9, 10).
- Steep HREE profiles in zircon indicate garnet breakdown, fluid influx, or melt-present conditions (Fig. 11).
- Both garnet and zircon (re)crystallization in the Alpine Schist are contemporaneous with the rifting of the Zealandia microcontinent from eastern Gondwana during 83 – 52 Ma (Fig. 5).
- South of Karangarua Rivzer, the transition from prograde to retrograde conditions occurs earlier than in the north. This area is closer in proximity to the Otago region which experienced extension from ~105 Ma onwards (Fig. 5).

LASS-ICP-MS Depth Profiling

- Enables the analysis of sub-micrometer, isotopically and/or geochemically distinct zircon domains which are too thin to be analyzed by other in situ methods (Fig. 12).
- Targets thin and discontinuous metamorphic zircon overgrowths capable of recording multiple short-duration tectonothermal events (Fig. 13).
- LASS depth-profile data linked to specific metamorphic events using zircon/garnet D_{REE} to discern the timing of garnet growth versus garnet breakdown (Fig. 7).
- 35 μm spot, continuous laser pulse at 2 Hz for 40 seconds, 80 pulses per depth-profile, ~8 μm deep.
- Rapid depth-profile analysis of ~350 detrital zircon grains.

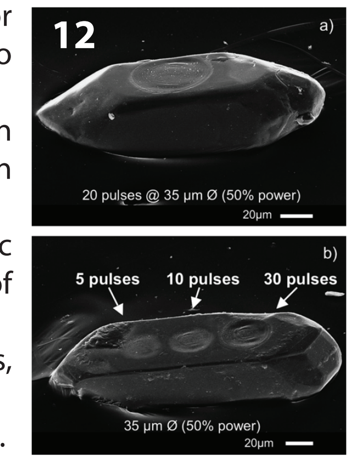

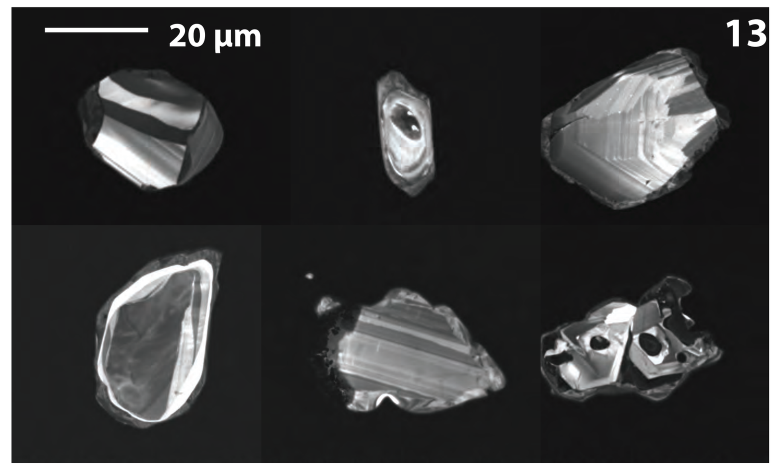

Fig. 12: SEM secondary electron images of ablation pits in Himalayan zircon analysed using the single-shot depth-profiling method [11].

Fig. 13: Cathodoluminescene images of Alpine Schist zircon analysed in this study using the continuous-pulse depth-profiling method. Rims range from <1 - 8 μm and show either turbid or oscillatory zoning.

Microcontinent formation

- The results of this study show that prograde conditions (contraction) in the outboard accretionary complex occurred simultaneously with extension and thinning in the inboard regions of the Gondwana margin during detachment of the Zealandia microcontinent.
- Numerical modeling of mantle wedge buoyancy [16] shows that gravitational collapse and detachment of microcontinents can be driven by stresses from the buoyancy of the mantle wedge once subduction ceases (Fig. 14).
- **Models predict that these stresses cause both extension in the overriding plate and shortening in the microcontinent** as it is pushed against the oceanic lithosphere.
- **The history of synchronous contraction and extension in Zealandia is consistent with these models, suggesting that the formation of the Zealandia microcontinent was driven by mantle wedge buoyancy (active) rather than passive orogenic collapse.**

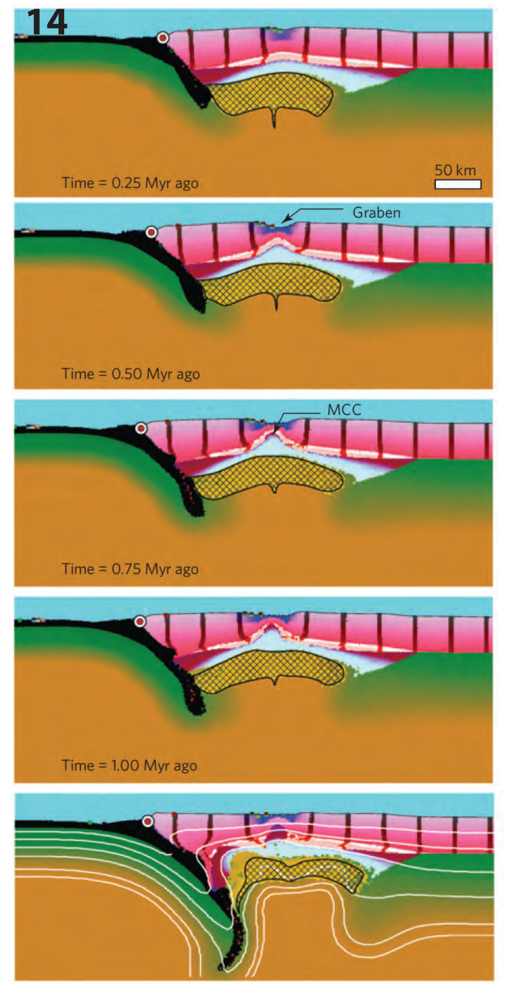

Fig. 14: Snapshots showing a time sequence of results from numerical modeling for an experiment with trench-normal velocity of 2.5 cm/yr [16]. Yellow hatched region is hydrated, partially molten (buoyant) mantle.

Fig. 15: Reconstructions of eastern Gondwana margin showing post-subduction plate reorganization [9]. Note slab roll back occurs only in NW Zealandia.